# Overview of NASA's Solar Electric Propulsion Project

## IEPC-2019-836

*Presented at the 36th International Electric Propulsion Conference*
*University of Vienna • Vienna • Austria*
*September 15 – 20, 2019*

Peter Y. Peterson[1], Daniel A. Herman[2], Hani Kamhawi[3], Jason D. Frieman[4], Wensheng Huang[4], Tim Verhey[4], Dragos Dinca[5], Kristen Boomer[6], Luis Pinero[4], and Kenneth Criswell[7]
*NASA Glenn Research Center, Cleveland, OH, 44135, United States*

Scott J. Hall[4] and Art Birchenough[6]
*Vantage Partners, NASA Glenn Research Center, Cleveland, OH, 44135, USA*

James H. Gilland[4]
*Ohio Aerospace Institute, NASA Glenn Research Center, Cleveland, OH, 44135, USA*

*and*

Richard Hofer[8], James E. Polk[9], Vernon Chaplin[9], Robert Lobbia[9], Charles E. Garner[10], and Matthew K. Kowalkowski[11]
*Jet Propulsion Laboratory, California Institute of Technology, Pasadena, CA, 91109, United States*

**Abstract: NASA is continuing to develop and qualify a state of the art 13 kW-class Advanced Electric Propulsion System (AEPS) for NASA exploration missions through a contract with Aerojet Rocketdyne (AR). An objective of the AEPS project is accelerate the adoption of high power electric propulsion technologies by reducing the risk and uncertainty of integrating Solar Electric Propulsion (SEP) technologies into space flight systems. NASA and AR have recently initiated testing of engineering hardware including the Hall Current Thruster (HCT), Power Processing Unit (PPU), and Xenon Flow Controller (XFC) at both the component and system levels. The successful completion of these tests will provide the required information to advance the AEPS system towards Critical Design Review. In support of the AEPS contract, NASA and JPL have been performing risk reduction activities to address specific concerns of this higher power Hall thruster propulsion system. These risk reduction activities have included long duration wear testing of the Technology Demonstration Unit (TDU) Hall thruster and cathode hardware, thermal cycling of TDU cathode heaters and coils, plasma plume measurements, and performed early circuit testing of the AEPS PPU design. In addition to the propulsion system development, the SEP project is developing the Plasma Diagnostic Package (PDP) and the SEP Testbed. The PDP is designed for use in conjunction with a high-powered electric propulsion (EP) system to characterize in-space operation. The SEP Testbed system is being developed to demonstrate**

[1] SEP Project Lead Engineer, NASA GRC Electric Propulsion System Branch, Peter.Y.Peterson@nasa.gov.
[2] PPE Ion Propulsion System Lead, NASA GRC Electric Propulsion Systems Branch, Daniel.A.Herman@nasa.gov.
[3] SEP Test Lead, NASA GRC Electric Propulsion Systems Branch, Hani.Kamhawi-1@nasa.gov.
[4] SEP Team Member, NASA GRC Electric Propulsion Systems Branch.
[5] SEP Power Processing Lead, NASA GRC Power Management and Distribution Branch, Dragos.Dinca@nasa.gov
[6] SEP Team Member, NASA GRC Power Management and Distribution Branch.
[7] SEP PDP Project Lead Engineer, NASA GRC Science And Space Technology Systems Branch, Kenneth.M.Criswell@nasa.gov
[8] SEP Thruster Lead, JPL Electric Propulsion Group, Richard.R.Hofer@jpl.nasa.gov.
[9] SEP Team Member, JPL Electric Propulsion Group.
[10] SEP AEPS System Engineering Lead, JPL Electric Propulsion Group, Charles.E.Garner@jpl.nasa.gov
[11] SEP AEPS XFC Lead, JPL Propulsion and Fluid Flight Systems Group, Matthew.K.Kowalkowski@jpl.nasa.gov

**integrated SEP system performance. The paper presents an overview of the NASA and the AEPS contract activities and a summary of the associated NASA in-house activities.**

## I. Introduction

NASA continues to evolve a human exploration approach for beyond low-Earth orbit and to do so, where practical, in a manner involving international, academic, and industrial partners [1]. Towards that end, NASA publicly presented a reference exploration concept at the Human Exploration and Operations Mission Directorate (HEOMD) Committee of the NASA Advisory Council meeting on March 28, 2017 [2]. This approach is based on an evolutionary human exploration architecture, expanding into the solar system with cislunar flight-testing and validation of exploration capabilities followed crewed missions.

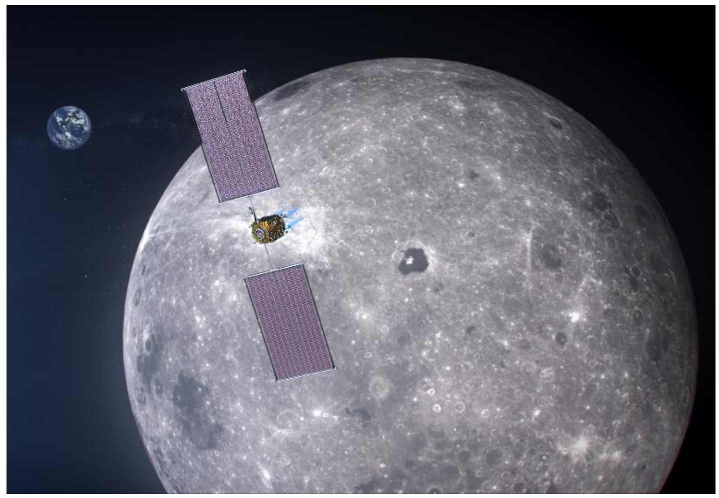

**Figure 1. NASA concept of the Power Propulsion Element (PPE) [Credits: NASA].**

The center of this approach is NASA's Gateway that is envisioned to provide a maneuverable outpost in Lunar orbit to extend human presence in deep space and expand on NASA exploration goals. The Gateway represents the initial step in NASA's architecture for human cislunar operations, lunar surface access and missions to Mars. NASA recently announced plans to send astronauts to the Lunar surface by 2024 as part of the newly formed Artemis program. A key enabling aspect of the Artemis program is the Gateway that provides access to the Moon surface. The first element of the Gateway is the Power and Propulsion Element (PPE), illustrated in Figure 1, in which NASA recently announced a commercial partnership to develop and demonstration a high-powered Solar Electric Propulsion (SEP) spacecraft with Maxar Technologies, formerly SSL [3]. The PPE will reach and maintain Lunar orbit by incorporating two high-powered SEP systems developed by NASA, in partnership with Aerojet Rocketdyne (AR), and Maxar [4]. The PPE is baselined to include two 13-kW Advanced Electric Propulsion Systems (AEPS) and four 6-kW Hall thrusters, currently under development by Maxar, for a total beginning of life propulsion power of over 60-kW [4].

High-power solar electric propulsion is one of the key technologies that has been prioritized because of its significant exploration benefits, specifically, for missions beyond low Earth orbit. Spacecraft size and mass are dominated by onboard chemical propulsion systems and propellants that may constitute more than 50 percent of spacecraft mass. This impact can be substantially reduced through the utilization of SEP, due to its higher specific impulse and lower propellant load required to meet the equivalent mission delta-V. Studies performed for NASA's HEOMD and Science Mission Directorate (SMD) have demonstrated that 40-kW-class SEP provides the necessary capabilities that would enable near term and future architectures, and science missions [5].

Accordingly, since 2012, NASA has been developing a 13-kW-class Hall thruster electric propulsion string that can serve as the building block for a 40-kW-class SEP capability. The 13-kW Hall thruster electric propulsion string development, led by the NASA Glenn Research Center (GRC) and the Jet Propulsion Laboratory (JPL), began with maturation of the high-power Hall thruster and Power Processing Unit (PPU). The technology development work has transitioned to AR via a competitive procurement selection for the AEPS contract in May, 2016. The AEPS Electric Propulsion (EP) string consists of the Hall Current Thruster (HCT), PPU (including digital control and interface functionality), Xenon Flow Controller (XFC), and associated intra-string harnesses. Management of the AEPS contract is being led by NASA GRC with funding from STMD. NASA continues to support the AEPS string development leveraging in-house expertise, plasma modeling capability, and world-class test facilities. NASA also executes risk reduction activities to support the AEPS string development and mission application.

The SEP project identified the need for improved plasma plume modeling integration of high-power EP systems with spacecraft, and for future extensibility of SEP into higher-powered missions [6]. This improved plasma plume modeling, then in turn, required reliable in-space plasma plume measurements for model validation, which resulted in the SEP project proposing and receiving approval to develop a Plasma Diagnostic Package (PDP) that would be flown on a PPE mission [7]. The SEP project also identified the need for an integrated high-power SEP spacecraft power systems for processing up to 60-kW. The SEP Testbed platform would be used to characterize the performance of integrated high-power SEP power systems.

## II. NASA's Solar Electric Propulsion Technology Development Status

This paper will highlight the recent progress with NASA SEP project's AEPS contract, NASA in-house risk reduction to support the AEPS string development and mission application, the development of the PDP hardware, and work conducted on the SEP Testbed.

### A. Advanced Electric Propulsion System Status

The AEPS contract includes the development, qualification, and delivery of two 13-kW electric propulsion strings qualified for flight. The AEPS EP string consists of the HCT, PPU (including digital control and interface functionality), XFC, string harnesses, and a command and data handling system for the safe operation of the AEPS string in ground based operation. The major components of the AEPS string are shown in Figure 2. The AEPS string is illustrated in Figure 3 for a typical spacecraft configuration.

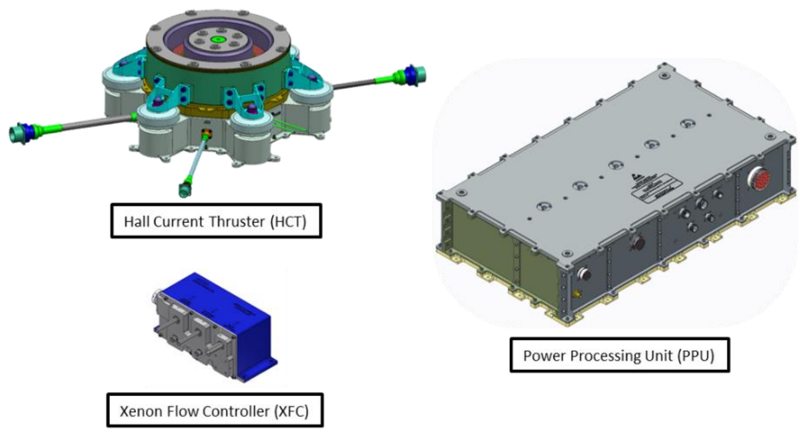


**Figure 2. The major components of the AEPS string (harness not shown).**

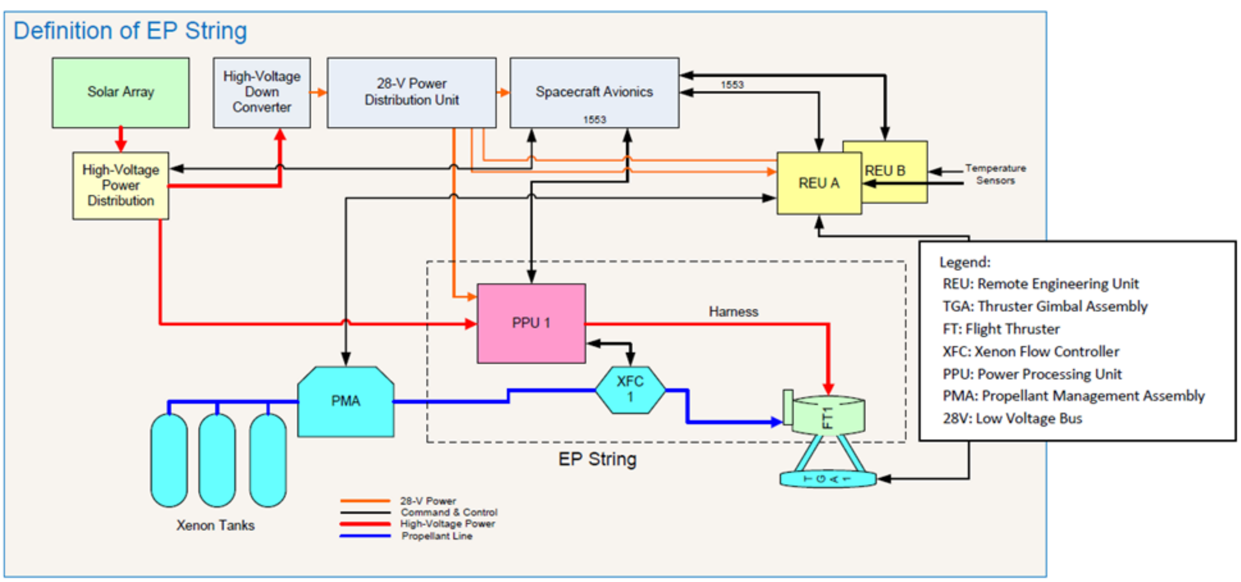


**Figure 3. AEPS string EP string definition, Ref. [8].**

The AEPS Special Test Equipment (STE), shown in Figure 4 consists of a load console, a core console, cabling, and breakout boxes. The load console simulates loads from the HCT and XFC when those components are not being tested. The core console contains all functionality required to operate the AEPS, including input power, signal conditioning, data acquisition, PPU test software and command and telemetry functions. During operation, the core console interfaces with the PPU, which can either drive the HCT and XFC to operate the full system or drive the load console to simulate system operation.

**Figure 4. AEPS STE under test with the Breadboard PPU**

AR has built upon the HERMeS thruster development investments to produce the HCT thruster design with improved structural capability, a modified thermal management approach that allows for elimination of the HERMeS thruster radiator, and improvements to manufacturability, including incorporation of a flight-qualified electromagnetic coil process. The AEPS HCT is designed to operate at input discharge powers up to 12.5 kW into the thruster, while providing a specific impulse over 2600 seconds at an input voltage of 600 volts. Figure 5 illustrates the design progression that the AEPS HCT has gone through to reach the final configuration that successfully completed acceptance testing.

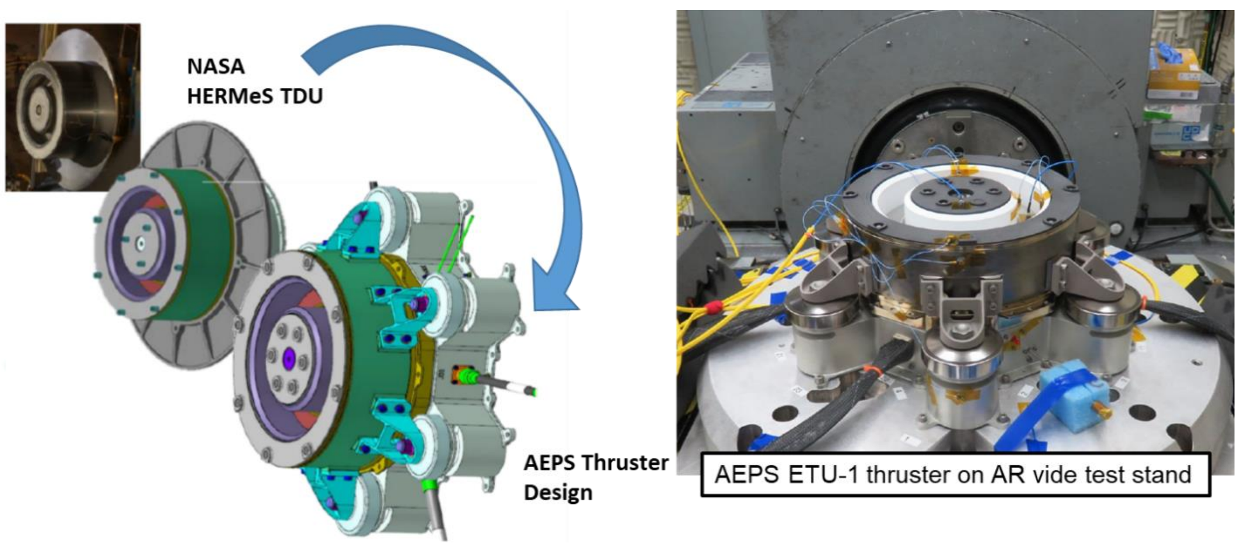


**Figure 5. AEPS design progression and Engineering Test Unit (ETU) thruster during vibration acceptance testing.**

The AEPS PPU leverages the work performed by NASA GRC on a brassboard power processor that was utilized in the integration testing of the HERMeS thruster [9]. The AEPS PPU provides discharge and subsystem power to the thruster, cathode keeper and heater, electromagnet coils, as well as XFC control, telemetry, system health monitoring, and spacecraft communications. The PPU is capable of providing nominal discharge currents up to 20.8 A for a discharge voltage output ranging from 300 to 600 V. The AEPS PPU is design to have power conversion efficiency up to 95% with a high-voltage input bus voltage ranging from 95 to 140V. The AEPS PPU mechanical packaging is shown in Figure 2.

The AEPS XFC is a derivative of the Xenon Flow Control Module that was previously developed under a NASA contract with VACCO [10]. The AEPS XFC is a highly integrated feed system that provides independent flow control to the anode and cathode, and provides pressure and flow rate monitoring on each propellant flow outlet. The AEPS XFC flow schematic and mechanical packaging is shown in Figure 6.

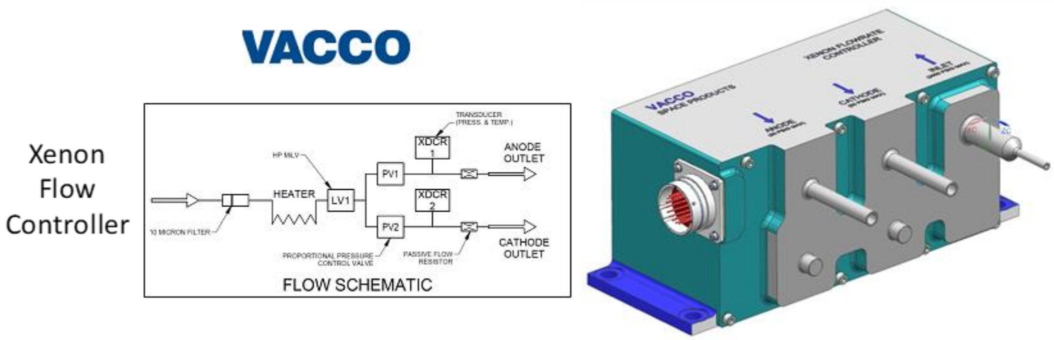


**Figure 6. AEPS VACCO XFC flow schematic and mechanical packaging.**

AR is currently completing fabrication of the two Engineering Test Unit (ETU) HCTs and will begin performance, plume, wear, and environmental testing in the fall of 2019. The ETU-1 HCT will undergo acceptance testing, followed by qualification level environmental testing at AR at JPL's Owens Chamber to assess the AEPS string (HCT, PPU, and XFC) prior to AEPS Critical Design Review (CDR). The ETU-1 environmental testing will include performance mapping, qualification level vibration and shock testing, and thermal vacuum testing of the AEPS ETU-1 HCT. The ETU-2 will be instrumented with thermal diagnostics, and thermal characterization testing will be performed in NASA GRC's Vacuum Facility-5. The ETU-2 will undergo extensive performance, stability, and plume characterization followed by Laser-Induced Fluorescence (LIF) mapping of the discharge plasma near the thruster exit plane. The ETU-2 LIF data will be compared to the HERMeS Technology Demonstration Unit (TDU) results and provide the HCT plasma models with discharge plasma data for model validation on AEPS hardware. Once the LIF mapping of the ETU-2 HCT is completed, the ETU-2 AEPS string will undergoing a long duration wear test prior to the AEPS CDR.

Fabrication of the ETU and Engineering Development Unit (EDU) PPUs are currently in-progress at AR. The ETU PPU will be used to assess the thermal characteristics of the PPU power modules and control boards in thermal desktop tests. Once completed the ETU PPU will be delivered to NASA for integration into a 1,000-hour string-level wear test of the ETU-2 HCT, ETU PPU, and EDU XFC. The EDU PPU will undergo full qualification-level environmental and performance characterization prior to being delivered to JPL for integration into a string-level thermal vacuum characterization of the ETU-1 HCT. Finally, two EDU XFCs will undergo full qualification-level environmental and performance characterization prior to be integrated in the EDT-1 and -2 string-level test campaigns. The results of the ETU and EDU component and string-level test campaigns will be used to provide final design improvements for the AEPS qualification/flight design.

### B. NASA SEP Project AEPS and Risk Reduction Status

#### *1. SEP AEPS PPU Risk Reduction Activities*

The AEPS PPU is one of three components that make up the AEPS electric propulsion string. The PPU provides regulated power to the HCT, controls the XFC, and serves as the communication interface between the AEPS EP string and the spacecraft. The PPU is designed to operate with an unregulated input bus of 95 Vdc to 140 Vdc. The Discharge Supply Unit (DSU) provides a continuously throttleable output voltage of 300 Vdc to 600 Vdc with a target efficiency of 95%. The DSU consists of four 3.3 kW power modules, for greater than 13 kW of regulated power to the HCT discharge. The closed loop controls for the DSU are implemented in the Discharge Master Control assembly, which also handles various hardware and software faults that are designed to protect the EP string. The PPU also provides regulated power to the HCT's heater, keeper, inner and outer magnets; the HCT ignition capability is included within the keeper power supply.

The AEPS PPU team consisting of Aerojet-Rocketdyne, ZIN Technologies, and NASA personnel have collaborated to develop this new state of the art PPU technology. In an effort to minimize AEPS PPU development risk, NASA has assembled a breadboard DSU and auxiliary power supplies (keeper, heater, and inner/outer magnet), in parallel with the contractor teams, and performed early circuit testing. The overall goal is to inform the team of various options to improve the PPU design robustness. The NASA contributions include: circuit design modifications to synchronize the power module startup with the pulse width modulation frequency to eliminate the generation of unsymmetrical pulses, ramp circuit modifications, transductor design testing, and other engineering design recommendations. These circuit design modifications, suggested by NASA GRC, have improved the robustness of the current PPU design. Figure 7 depicts the breadboard AEPS power modules tested at NASA GRC (power module testing and heater power supply testing).

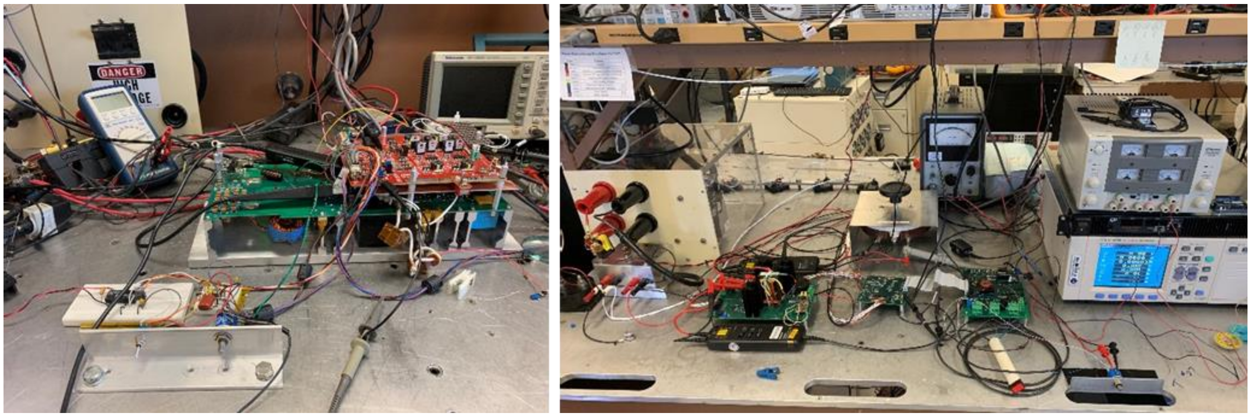

**Figure 7. NASA breadboard power modules used for AEPS risk reduction activities.**

### *2. Long Duration Wear Test*

As part of its risk reduction activities, NASA has conducted a series of wear tests to identify erosion phenomena and the accompanying failure modes, as well as to validate service-life models for magnetically shielded thrusters. The third of these wear tests (named the TDU-3 Long Duration Wear Test) began in October 2017 and was completed in October 2018 [11, 12]. The overall goal of this test was to quantify performance, stability, plume, and wear trends of TDU-3 over a minimum of 3,000 hours of operation. In addition to providing erosion data, the TDU-3 long duration wear test served as a pathfinder for the planned life and qualification testing of the hardware to be delivered as part of the AEPS contract, as well as two new diagnostics: a thrust vector probe and in-situ wear tool [13, 14].

Similar to the approach taken in previous TDU wear tests, the TDU-3 wear test was periodically interrupted to acquire performance, stability, and plume data for a set of six Reference Firing Conditions (RFC). The thrust of TDU-3, measured at each RFC is shown as a function of total operating time in Figure 8. The measured thrust of TDU-3, during the long duration wear test, varied by less than the thrust stand uncertainty (±5 mN) for all RFCs. Similar invariance (less than the thrust stand uncertainty) was also observed for the discharge current oscillations and plume properties [11, 12].

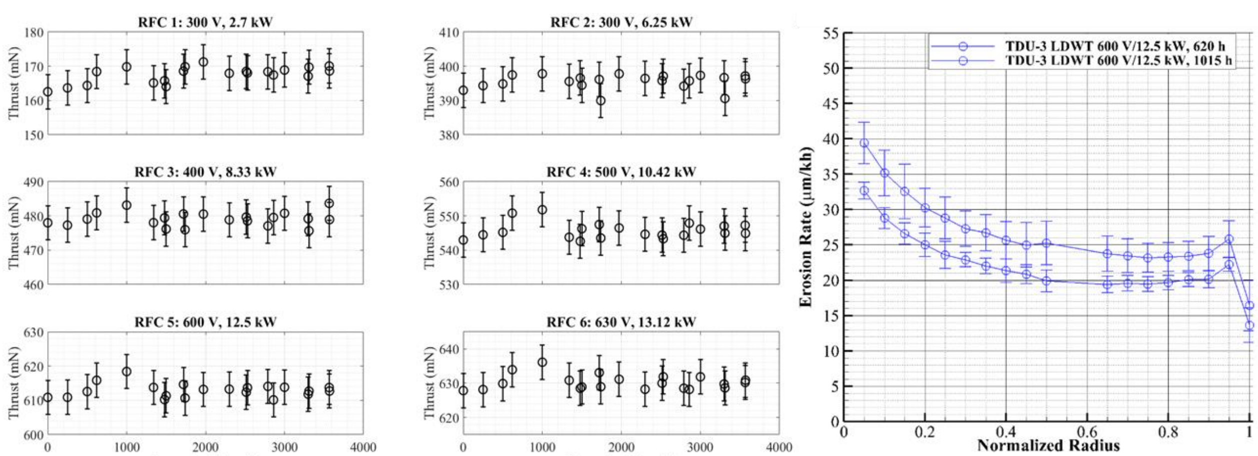


**Figure 8. TDU-3 thrust as a function of operating time during the LDWT and IFPC erosion rates measured during Segment I of the TDU-3 LDWT.**

Previous TDU wear tests identified the Inner Front Pole Cover (IFPC), Outer Front Pole Cover (OFPC), and cathode keeper as the most likely life-limiting components for HERMeS[15]. Sample IFPC erosion rates measured during the long duration wear test are shown in Figure 8. Using the worst-case wear measurements for the IFPC erosion rates, there is more than 40% lifetime margin, relative to the maximum, allowable IFPC erosion rate of 88 µm/kh for operation at 600 V/12.5 kW. Larger lifetime margins, of approximately 80% were observed for both the OFPC and keeper.

Overall, the TDU-3 long duration wear test successfully served as a pathfinder for the planned life and qualification testing of AEPS hardware. The HERMeS thruster design was shown to offer consistent performance over more than 3500 h of operation, while exhibiting component lifetime margins of greater than 40% at the nominal 600 V/12.5 kW operating condition. The opportunity afforded by the long duration wear test, to develop this experience with long duration testing of high-power Hall thrusters, will significantly lower the risks of erosion for future extended duration tests including the planned AEPS qualification effort.

### *3. Laser-Induced Fluorescence Testing and Thruster Modeling*

In preparation for AEPS thruster testing at NASA, a new Laser-Induced Fluorescence (LIF) diagnostic was implemented and checked out on the HERMeS TDU-1 thruster at GRC [16]. The goal of the new LIF diagnostic is to map, near the exit channel, ion velocity distribution and directions, and use the data for thruster plasma model validation that be used in the qualification process of the AEPS thruster [17]. The new LIF system at GRC compliments the LIF capabilities at JPL [18, 19] and will provide necessary HCT data for the validation of the thruster modeling simulation [20-22]. Time-average and time-resolved LIF measurements have been used to provide insights in the evolution of the ion velocity distribution function providing critical validation for the plasma models as shown in Figure 9.

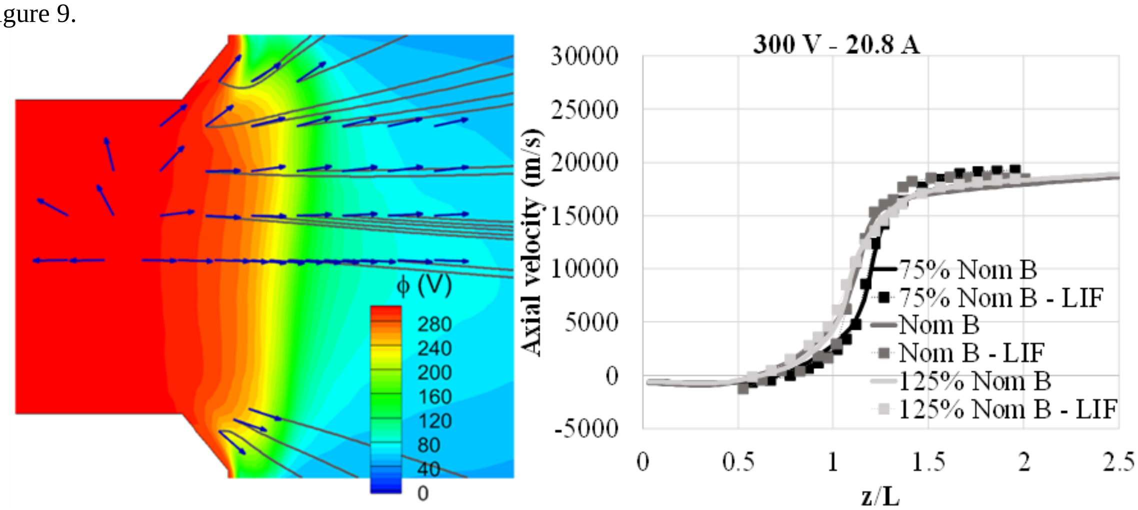


**Figure 9. Left: 2-D comparison between singly charged ion streamlines from JPL's Hall2De and unit vectors of the ion velocity field from LIF measurements at nominal magnetic field strength. The velocity fields are overlaid on the computed contours of the plasma potential. Right. Comparison of the LIF and computed axial ion velocities along the channel centerline at different strengths of the magnetic field.**

The new GRC LIF laser setup uses three laser axes to provide definitive correlation ion velocity populations. The LIF functional checkout test generated a complete set of ion velocity distribution function maps of the TDU-1 across various discharge voltages, discharge powers, magnetic field strengths, and background pressures. A low-energy ion population, independent of the beam ions, was measured near the edge of the ion beam exiting the discharge channel. Comparison of the LIF data with the retarding potential analyzer data confirmed the presence of these low-energy ions towards the sides of the thruster (70-90° from the firing axis) in the far field with energies up to 200 eV, which in not sufficient to account for the observed front pole erosion. Figure 10 show the averaged velocity vectors near the discharge channel, IFPC, and OFPC, respectively, for the TDU-1 operating at 300 V, 6.3 kW.

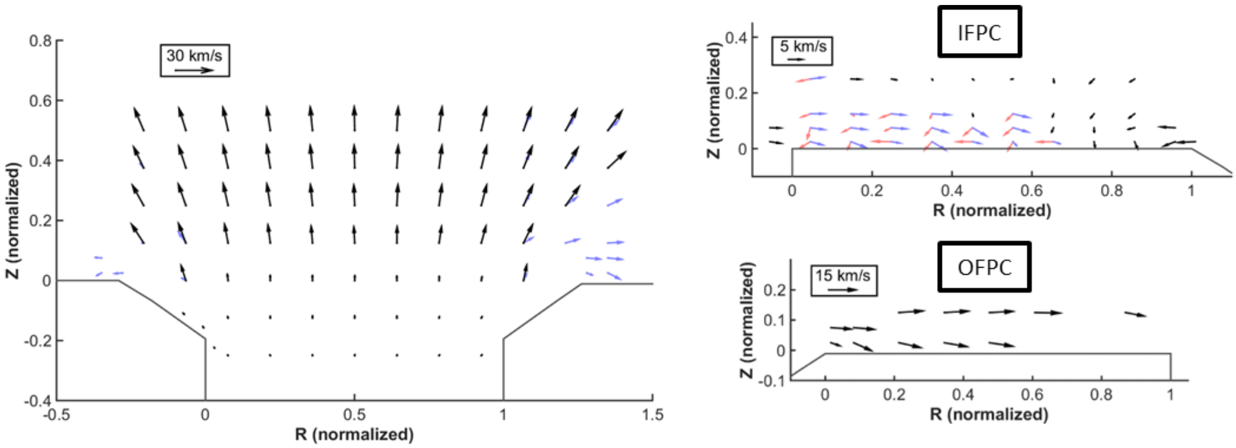


**Figure 10. Averaged velocity vector near the discharge channel, IFPC, and OFPC for 300 V, 6.3 kW operation. Right: The black arrows represent the beam ions while the blue arrows represent the low-energy ions. Left: the red arrows represent the discharge channel stream while the blue arrows represent the cathode stream ions.**

***4. Cathode Risk Reduction***

A critical component of the AEPS thruster is a centrally mounted hollow cathode, which generates the charged particles necessary for efficient operation of this thruster. Building off the extensive history of cathode development at NASA and AR, development hollow cathodes were fabricated for use in the NASA HERMeS thruster wear-tests in 2016-2019 and a series of extended duration cathode tests [11, 12, 23, 24]. This cathode design, referred to as the Mark II, was a more flight-like design, compatible with the AEPS thruster. Fabrication of the Mark II cathodes began at NASA in early 2018 with the first unit completing assembled in May 2018. Three Mark II cathodes have been successfully operated in small vacuum chambers at NASA GRC and JPL.

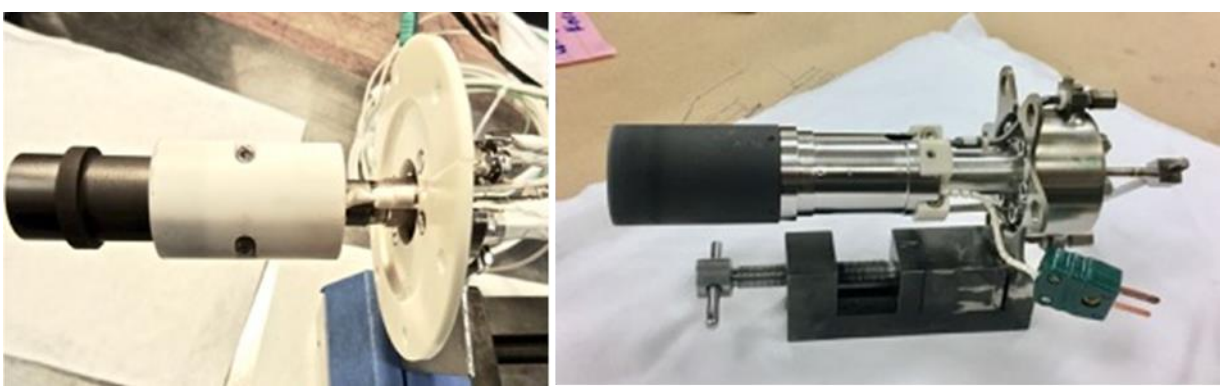

**Figure 11. NASA hollow cathodes used in AEPS/HERMeS HCT testing. A) Technology Demonstration Unit cathode and B) Mark II design.**

In addition to the TDU cathodes, the SEP team at NASA and JPL is supporting risk reduction testing of the AEPS hollow cathodes through a series of component tests:

- Swaged heaters fabricated at AR will be tested at NASA JPL to verify life capability through cyclic testing over an equivalent thermal range that the component will be expected to see in-space. Multiple heaters are to be tested for component verification.
- An EDU cathode will be cyclically tested at JPL to three times the cycle life requirement of the cathode and cathode heater. The cathode will be ignited and operated during each cycle to verify operating capability. Additionally, the cathode will be thermally cycled through the temperature range expected in-space to ensure compatibility with the space environment.
- A second EDU cathode will be operated at GRC for the full duration of the mission requirement to verify cathode capability through end of life.

- All AEPS cathodes will be tested in magnetic field simulators to ensure the hollow cathode will experience a thruster-like environment.

Data collected from the cathode component level and the thruster life tests will be combined to provide the information needed to verify life capabilities of the AEPS cathode within high-power Hall thrusters.

### 5. *Magnetic Field Optimization*

During the design phase of the HERMeS thruster, the approach was to design a magnetic circuit that incorporated the lessons learned from the H6MS and the NASA-300MS thruster work [25, 26]. The TDU magnetic field topology was shielded to assure that discharge channel erosion was eliminated. This was validated by the wall probe test that was performed at discharge voltages up to 800 V [27]. The wear tests of the HERMeS TDU-1, -2, and -3 thrusters found that discharge erosion rates were minimized; however, measurable erosion of the front pole covers, although lower than discharge channel erosion rates of unshielded thrusters, was found to be the next life-limiting mechanism [11, 12, 28-30]. The objectives of the magnetic field optimization tests were to evaluate several candidate magnetic field topologies in an effort to find a balance between discharge channel erosion and front pole erosion while maintaining the performance and stability of the HERMeS thruster and meeting the lifetime requirements for high-power NASA SEP mission concepts.

Magnetic field optimization tests were performed on the TDU-1 Hall thruster. Three candidate magnetic field topologies (B1, B2 and B4) were designed, modeled, and tested. Testing of the candidate magnetic field topologies was performed at the NASA GRC Vacuum Facility 6 in two phases. During Phase I, LIF measurements were performed on the baseline (B0) and candidate magnetic field topologies (B1, B2, and B4). In Phase II, the performance, stability, wear (except for B4), plasma plume, and optical emission spectroscopy measurements were performed to provide data to assess the optimal configuration. Figure 12 shows the thrust efficiency during thruster operation at 12.5 kW and a discharge voltage of 600 V. Results in Figure 12 indicate that within the uncertainty of the measurement, the performance of the B0 and B2 configurations is almost identical across the various magnetic field settings of the thruster. Figure 12 also presents the normalized discharge current RMS magnitudes during the magnetic mapping test. These results show that, in general, the B2 configuration attained lower discharge current oscillation levels than B0, B1, and B4 configurations. The wear test results found that inner front pole cover erosion rates of configurations B1 and B2 were on average 65% and 39% lower, respectively, than that of the baseline configuration B0. Additional details of the magnetic field optimization testing can be found in Ref [28].

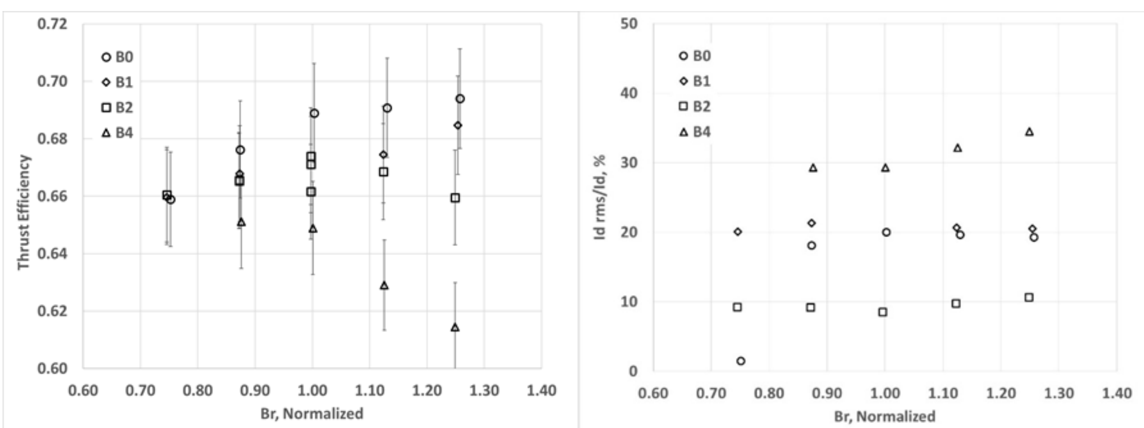


**Figure 12. Magnetic Field Optimization performance and stability results for the TDU-1 operating at 12.5 kW and 600 V. Left: Thrust efficiency for B0, B1, B2, and B4 configurations. Right: Normalized discharge current RMS for B0, B1, B2, and B4 configurations.**

## C. Plasma Diagnostic Package Status

A flight PDP, being developed by NASA GRC, will be delivered to Maxar as Government Furnished Equipment (GFE) for inclusion on the PPE [4, 7]. The PDP will provide the data needed to validate models of high-power SEP operation and spacecraft plasma interactions, design tools that are critical for enabling high-power SEP spacecraft to support future human and robotic missions to Mars. The PDP will collect in-space plasma plume data from the PPE Ion Propulsion System (IPS). All IPS thrusters emit high-energy ions in a plasma plume that provides the spacecraft thrust. These plasma plume ions can be harmful to spacecraft by causing erosion and contamination of spacecraft surfaces with back-sputter erosion products. These thruster plasma plume characteristics are measured in ground based vacuum chambers. Unfortunately, the current computer simulated models cannot be validated for in-space plasma plume characteristics accurately due to the limitation of vacuum facility pumping speeds to achieve space like vacuum and the potential interaction of the facility with the plasma plume [31-39]. PDP in-space data is necessary to mitigate the risks of plasma plume interaction for PPE and Gateway [8].

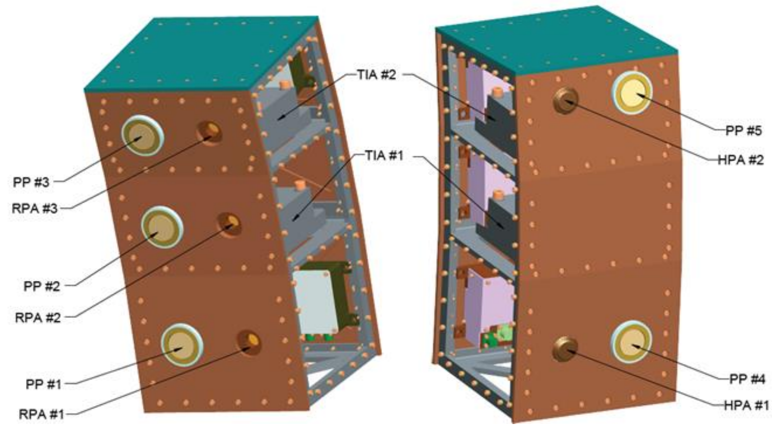


**Figure 13. Concept of the PDP Thruster Probe Assembly (TPA).**

The PDP consist of a Thruster Probe Assembly (TPA), Main Electronic Package (MEP), and associated harnesses. The TPA, shown in Figure 13, has ten sensors with three sets of duplicate sensors at different angular positions facing an AEPS thruster and two sets facing away from the AEPS thruster. The MEP serves as the avionics for the TPA data collection and communication link to the PPE spacecraft. The TPA notional location on the PPE spacecraft, shown in Figure 14, is important consideration due to the sensor design specifications and the avionics capabilities.

Once NASA successfully completes an integrated functional system test of the PDP, the PDP flight hardware will be delivered to Maxar for integration into the PPE spacecraft. A concept of operations and interface control documents will be developed by NASA and Maxar. Once operational on PPE, PDP data will provide NASA and Maxar invaluable plasma plume characteristics of high-power SEP in a space environment. This knowledge will improve the accuracy and confidence in future computer models and ultimately the extensibility of SEP to even higher power levels needed for human exploration.

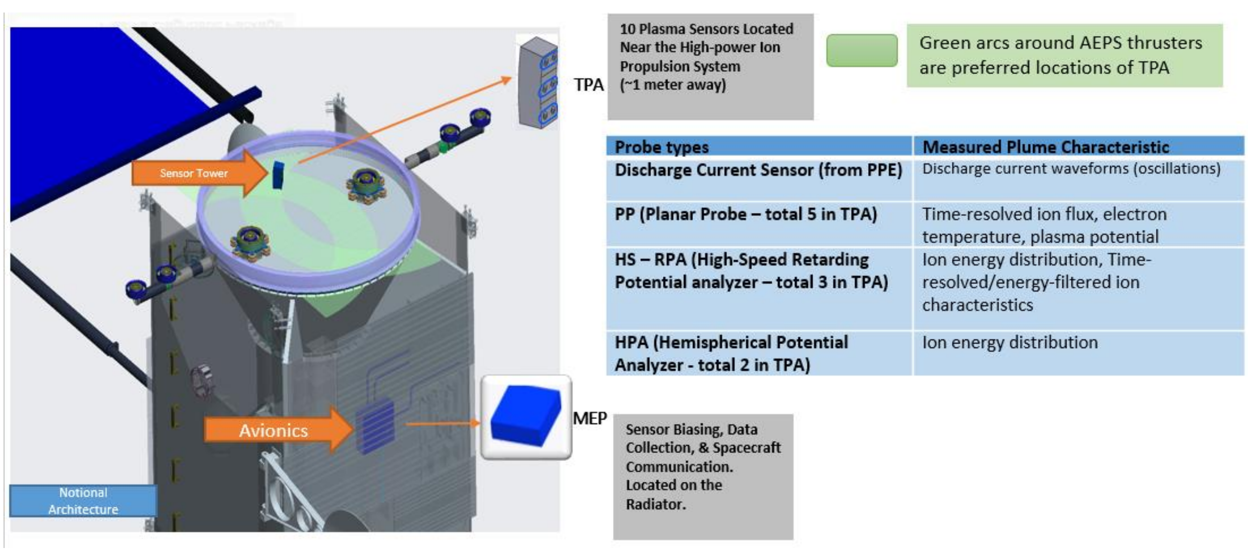


**Figure 14. Notional PDP location on the PPE concept spacecraft.**

### D. Testbed Status

The SEP Testbed is a modular and reconfigurable testbed designed to meet the needs of current and future SEP missions by providing an end-to-end evaluation and test capability for SEP systems. The testbed provides a platform to characterize the performance of integrated high-power SEP power systems up to 60kW. Hardware consists of high and low voltage power sources, a high voltage power distribution unit (HVPDU), up to four EP strings or EP string simulators, a spacecraft load simulator, up to two visiting vehicle load simulators, and a command and data handling (C&DH) system. The SEP Testbed was designed to accommodate various fidelities of hardware from breadboard to flight hardware. Interfaces compatible with flight hardware were qualified to NASA-STD-5005D, “Standard for the Design and Fabrication of Ground Support Equipment.”

The high voltage power source for the SEP Testbed consists of either a commercial-off-the-shelf power supply or a Solar Array Electrical Simulator (SAES) developed by NASA GRC. The SAES design is based on a heritage design from the International Space Station (ISS). The unit consists of 60 strings, each with an open circuit voltage capability up to 180V and a short circuit current capability up to 6.5A, and has the capability to re-program the curve to simulate the solar array, depending on the mission requirements. The full-power configuration of the testbed would include two SAES units. The HVPDU receives unregulated high voltage power from the source and distributes it to the various loads through latching contactors. The EP string loads consist of a PPU, XFC, and a thruster or thruster simulator. The PPUs presently used in the SEP Testbed were designed and built at NASA GRC under a past NASA STMD project and have an input voltage range of 95-140 VDC and an output voltage range of 300-800 VDC [40]. The spacecraft load simulator represents the electrical interface at the input of a high voltage to low voltage converter, which would supply power to the various spacecraft low voltage electrical loads. The visiting vehicle interface load simulator represents the electrical power consumed by a visiting vehicle docked to a SEP spacecraft. The C&DH consists of a control system and data acquisition system, providing an interface for an operator to monitor and control the SEP Testbed hardware and interfaces.

The SEP Testbed was designed to be built at NASA GRC in a phased approach, gradually increasing the power level and fidelity of the testbed. Phases 1 and 2A were completed as of the end of FY18. Each phase consists of integration testing to verify that the testbed requirements are satisfied and all interfaces are configured properly, followed by risk reduction testing, consisting of power quality tests to demonstrate system stability and transient performance over a range of operating conditions. Phase 1 integrated the heritage ISS SAES with the HVPDU, a single 14kW EP string load consisting of the GRC-built PPU and HCT thruster simulator load bank, a converter representative of the spacecraft load, and the C&DH. Phase 2A incorporated the SEP SAES, a second identical EP string load, and an updated C&DH. Power quality tests were run at various power levels in each phase, using the International Space Power System Interoperability Standard as a baseline. Examples of data collected includes noise, ripple, and load steps. Proposed future phases would include further increasing the fidelity of hardware and moving to a facility to interface with a HCT. Figure 15 shows a diagram of the SEP Testbed hardware configuration by phase.

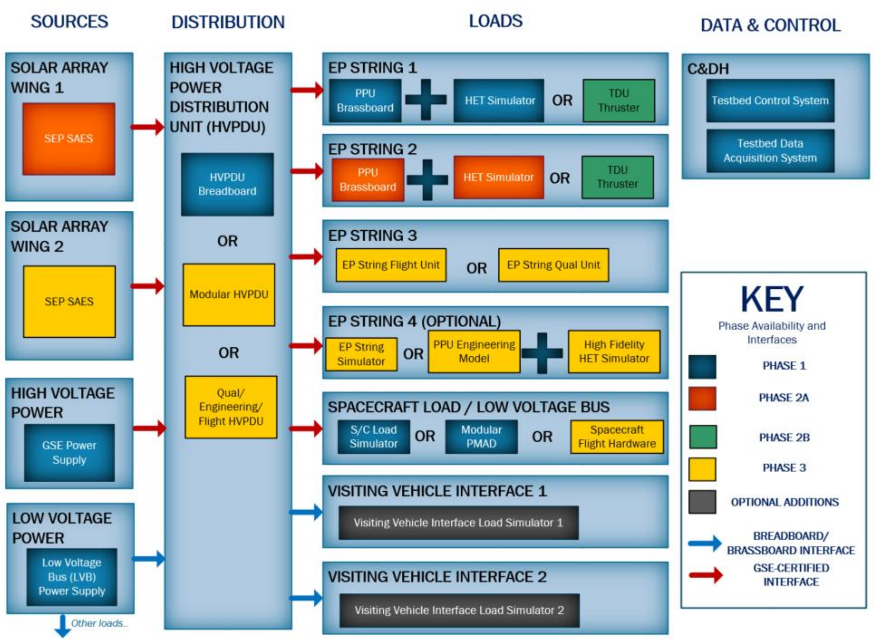


**Figure 15. SEP Testbed Hardware Configuration by Phase.**

## III. Conclusion

NASA is committed to the development and application of high power solar electric propulsion as a key element of future human exploration plans and returning humans to the Lunar surface. The recent selection of Maxar to build, launch, and operate the PPE prior to delivering the element to NASA for Gateway has proven that SEP is capable and ready to provide NASA a means of accomplishing difficult exploration missions. The AEPS contract development represents a continuation of STMD-funded efforts first initiated with the in-house, collaborative HERMeS thruster and HP-120V PPU developments conducted by NASA GRC and JPL. Ongoing advanced technology development work is being performed by AR under the AEPS contract is managed by NASA GRC. Under the AEPS contract, AR will qualify the AEPS for use on NASA missions. The NASA SEP project is continuing the development of the PDP for use on the PPE spacecraft. The plasma plume data from the PDP will provide invaluable data form SEP plume modelers and SEP integration into future NASA missions. The NASA Testbed is a valuable tool for spacecraft integration studies on spacecraft power and SEP systems.

## Acknowledgments

The authors would like to thank the Space Technology Mission Directorate through the Solar Electric Propulsion Technology Demonstration Mission Project for funding the joint NASA GRC and JPL development of the Advanced Electric Propulsion System. The authors would also like to thank the many NASA/Aerojet team members and subject matter experts for providing their expertise and technical guidance in the development of AEPS, PDP, and Testbed.

## IV. References

[1] Congress, "National Aeronautics and Space Administration Transition Authorization Act of 2017," ed, 2017.

[2] W. Gerstenmaier, "Progress in Defining the Deep Space Gateway and Transport Plan," in *NASA Advisory Council Human Exploration and Operations Committee Meeting*, Washington, DC, 2017.

[3] NASA. (2019). *NASA Awards Artemis Contract for Lunar Gateway Power, Propulsion* Available: https://www.nasa.gov/press-release/nasa-awards-artemis-contract-for-lunar-gateway-power-propulsion

[4] R. Ticker, M. Gates, D. Manzella, A. Biaggi-Labiosa, and T. Lee, "The Gateway Power and Propulsion Element: Setting the Foundation for Exploration and Commerce," presented at the 2019 Joint Propulsion Conference, Indianapolis, IN, 2019.

[5] B. K. Smith, M. L. Nazario, and C. C. Cunningham, "Solar Electric Propulsion Vehicle Demonstration to Support Future Space Exploration Missions," presented at the Space Propulsion 2012, Bordeaux, France, 2012.

[6] D. A. Herman, W. Santiago, H. Kamhawi, J. E. Polk, J. S. Snyder, R. R. Hofer, and M. J. Sekerak, "The Ion Propulsion System for the Asteroid Redirect Robotic Mission," presented at the 52nd AIAA/SAE/ASEE Joint Propulsion Conference, 2016.

[7] NASA. (2019). *Spaceflight Demonstration of a Power and Propulsion Element (PPE)*. Available: https://www.fbo.gov/spg/NASA/GRC/OPDC20220/80GRC018R0005/listing.html

[8] D. A. Herman, W. Santiago, H. Kamhawi, J. E. Polk, J. S. Snyder, R. R. Hofer, and M. Parker, "The Ion Propulsion System for the Asteroid Redirect Robotic Mission," in *52nd AIAA/SAE/ASEE Joint Propulsion Conference*, Salt Lake City, UT, 2016.

[9] W. Santiago, K. E. Bozak, L. R. Pinero, R. J. Scheidegger, M. C. Gonzalez, A. G. Birchenough, M. J. Garrett, and N. V. Ivanov, "High Input Voltage, Power Processing Unit Performance Demonstration," presented at the 52nd AIAA/SAE/ASEE Joint Propulsion Conference, AIAA-2016-5033, Salt Lake City, UT, 2016.

[10] J. M. Cardin, W. Cook, and R. Bhandari, "Qualification of an Advanced Xenon Flow Control Module," in *33rd International Electric Propulsion Conference*, Washington, DC, 2013.

[11] J. D. Frieman, H. Kamhawi, J. Mackey, T. Haag, P. Peterson, D. Herman, and J. H. Gilland, "Completion of the Long Duration Wear Test of the NASA HERMeS Hall Thruster," presented at the 2019 Joint Propulsion Conference, Indianapolis, IN, 2019.

[12] J. D. Frieman, H. Kamhawi, G. Williams, W. Huang, D. Herman, P. Peterson, and J. H. Gilland, "Long Duration Wear Test of the NASA HERMeS Hall Thruster," presented at the 2018 Joint Propulsion Conference, AIAA-2018-4645, Cincinnati, OH, 2018.

[13] G. F. Benavides, J. Mackey, D. M. Ahern, and R. Thomas, "Diagnostic for Verifying the Thrust Vector Requirement of the AEPS Hall-Effect Thruster and Comparison to the NEXT-C Thrust Vector Diagnostic," presented at the 2018 Joint Propulsion Conference, AIAA-2018-4514, Cincinnati, OH, 2018.

[14] D. M. Ahern, J. D. Frieman, G. Williams, J. Mackey, T. Haag, W. Huang, and H. Kamhawi, "In-situ Diagnostic for Assessing Hall Thruster Wear," presented at the 2018 Joint Propulsion Conference, AIAA-2018-4721, Cincinnati, OH, 2018.

[15] E. Vietzke, A. Refke, V. Philipps, and M. Hennes, "Energy Distributions and Yeilds of Sputtered $C_2$ and $C_3$ Clusters," *Journal of Nuclear Materials*, pp. 810-815, 1997 1997.

[16] W. Huang, H. Kamhawi, and D. Herman, "Ion Velocity in the Discharge Channel and Near-Field of the HERMeS Hall Thruster," presented at the 2018 Joint Propulsion Conference, AIAA-2018-4723, Cincinnati, OH, 2018.

[17] J. Polk and J. Brophy, "Life Qualication of Hall Thrusters By Analysis andTest," presented at the Space Propulsion 2018 Conference, 00547, Seville, Spain, 2018.

[18] V. Chaplin, "Spatiotemporally Resolved Ion Velocity Distribution Measurements in the 12.5 kW HERMeS Hall Thruster," presented at the 36th International Electric Propulsion Conference, University of Vienna, Austria, 2019.

[19] V. H. Chaplin, B. A. Jorns, A. Lopez Ortega, I. G. Mikellides, R. W. Conversano, R. B. Lobbia, and R. R. Hofer, "Laser-induced fluorescence measurements of acceleration zone scaling in the 12.5 kW HERMeS Hall thruster," *Journal of Applied Physics*, vol. 124, 2018.

[20] A. Lopez Ortega, I. G. Mikellides, M. J. Sekerak, and B. A. Jorns, "Plasma simulations in 2-D (r-z) geometry for the assessment of pole erosion in a magnetically shielded Hall thruster," *Journal of Applied Physics*, vol. 125, 2019.

[21] A. Lopez Ortega, I. Mikellides, and D. M. Goebel, "Numerical Simulations for Life Assessments of the BaO and LaB6 Cathode Options in the Hall Effect Rocket with Magnetic Shielding (HERMeS)," presented at the 35$^{th}$ International Electric Propulsion Conference, Atlanta, GA, 2017.

[22] A. Lopez Ortega, I. Mikellides, and V. Chaplin, "Numerical Simulations for the Assessment of Erosion in the 12.5-kW Hall Effect Rocket with Magnetic Shielding (HERMeS)," presented at the 35$^{th}$ International Electric Propulsion Conference, IEPC-2017-154, Atlanta, GA, 2017.

[23] P. Y. Peterson, J. D. Frieman, H. Kamhawi, G. Williams, J. H. Gilland, R. Hofer, and D. Herman, "NASA HERMeS Hall Thruster Long Duration Wear Test," presented at the 65th JANNAF Propulsion Meeting, Long Beach, CA, 2018.

[24] T. R. Verhey, H. Kamhawi, D. M. Goebel, J. E. Polk, P. Y. Peterson, and D. A. Robinson, "Hollow Cathode Assembly Development for the HERMeS Hall Thruster," in *52$^{nd}$ AIAA/SAE/ASEE Joint Propulsion Conference*, Salt Lake City, UT, 2016.

[25] R. R. Hofer, D. M. Goebel, I. G. Mikellides, and I. Katz, "Magnetic shielding of a laboratory Hall thruster. II. Experiments," *Journal of Applied Physics*, vol. 115, Jan 28 2014.

[26] H. Kamhawi, W. Huang, T. W. Haag, R. Shastry, G. C. Soulas, T. B. Smith, I. Mikellides, and R. R. Hofer, "Performance and Thermal Characterization of the NASA-300MS 20 kW Hall Effect Thruster," in *33rd International Electric Propulsion Conference*, Washington, DC, 2013.

[27] R. Shastry, W. Huang, and H. Kamhawi, "Near-Surface Plasma Characterization of the 12.5-kW NASA TDU1 Hall Thruster," presented at the To be Presented at the 51st AIAA/SAE/ASEE Joint Propulsion Conference, Orlando, FL, 2015.

[28] H. Kamhawi, "Performance, Plume, Stability,and Wear Characterization of Three Alternate Magnetic Field Topologies in the Hall Effect Rocket with Magnetic Shielding," presented at the 36$^{th}$ International Electric Propulsion Conference, IEPC-2019-902, Vienna, Austria, 2019.

[29] G. J. Williams, J. H. Gilland, P. Y. Peterson, H. Kamhawi, W. Huang, M. Swiatek, C. Joppeck, J. Yim, and T. W. Haag, "Wear Testing of the HERMeS Thruster," presented at the 52$^{nd}$ AIAA/SAE/ASEE Joint Propulsion Conference, AIAA-2016-5025, Salt Lake City, UT, 2016.

[30] J. E. Polk, R. B. Lobbia, A. Barriault, V. Chaplin, A. Lopez-Ortega, and I. Mikellides, "Inner Front Pole Erosion in the 12.5 kW HERMeS Hall Thruster Over a Range of Operating Conditions," presented at the 35$^{th}$ International Electric Propulsion Conference, IEPC-2017-409, Atlanta, GA, 2017.

[31] P. Y. Peterson, H. Kamhawi, W. Huang, G. Williams, J. Gilland, J. Yim, R. R. Hofer, and D. Herman, "NASA's HERMeS Hall Thruster Electrical Configuration Characterization," presented at the 52nd AIAA/ASME/SAE/ASEE Joint Propulsion Conference, AIAA-2016-5027, Salt Lake City, UT, 2016.

[32] I. Katz, A. Lopez Ortega, D. Goebel, M. Sekerak, R. Hofer, and B. Jorns, "Performance and Facility Background Pressure Characterization Tests of NASA’s 12.5-kW Hall Effect Rocket with Magnetic Shielding Thruster," in *14th Spacecraft Charging Technology Conference, ESA/ESTEC,*, Noordwijk, NL USA, 2016.

[33] H. Kamhawi, T. W. Haag, W. Huang, D. A. Herman, G. J. Williams, P. Y. Peterson, R. R. Hofer, and I. Mikellides, "Performance, Stability, and Pressure Effects Characterization Tests of NASA’s 12.5-kW Hall Effect Rocket with Magnetic Shielding (HERMeS) Thruster," in *52$^{nd}$ AIAA/SAE/ASEE Joint Propulsion Conference*, Salt Lake City, UT, 2016.

[34] W. G. Tighe, R. Spektor, and K. D. Diamant, "Effects of Background Pressure on the NASA 173M Hall Current Thruster Performance," presented at the 34th International Electric Propulsion Conference, Kobe, Japan, 2015.

[35] H. Kamhawi, W. Huang, T. Haag, R. Shastry, R. E. Thomas, J. T. Yim, D. A. Herman, G. Williams, J. Myers, R. R. Hofer, I. Mikellides, M. J. Sekerak, and J. E. Polk, "Performance and Facility Background Pressure Characterization Tests of NASA's 12.5-kW Hall Effect Rocket with Magnetic Shielding Thruster," presented at the 34th International Electric Propulsion Conference, Kobe, Japan, 2015.

[36] W. Huang, H. Kamhawi, R. B. Lobbia, and D. L. Brown, "Effect of Background Pressure on the Plasma Oscillation Characteristics of the HiVHAc Hall Thruster," presented at the 50th AIAA/ASME/SAE/ASEE Joint Propulsion Conference, Cleveland, OH, 2014.

[37] R. R. Hofer and J. R. Anderson, "Finite Pressure Effects in Magnetically Shielded Hall Thrusters," presented at the 50th AIAA/ASME/SAE/ASEE Joint Propulsion Conference, Cleveland, OH, 2014.

[38] K. D. Diamant, R. Liang, and R. L. Corey, "The Effect of Background Pressure on SPT-100 Hall Thruster Performance," in *50th AIAA/ASME/SAE/ASEE Joint Propulsion Conference and Exhibit, AIAA-2014-3710*, Cleveland, OH, USA, 2014.

[39] K. D. Diamant, R. Spektor, E. J. Beiting, J. A. Young, and T. J. Curtiss, "The Effects of Background Pressure on Hall Thruster Operation," in *48th AIAA/ASME/SAE/ASEE Joint Propulsion Conference and Exhibit, AIAA-3735-2012*, Atlanta, Georgia, USA, 2012.

[40] L. R. Pinero, K. E. Bozak, W. Santiago, R. J. Scheidegger, and A. G. Birchenough, "Development of High-Power Hall Thruster Power Processing Units at NASA GRC," presented at the 51st AIAA/SAE/ASEE Joint Propulsion Conference, Orlando, FL, 2015.